On the potential of using nanocellulose for consolidation of painting canvases

Oleksandr Nechyporchuk [a,1,*], Krzysztof Kolman [a,2], Alexandra Bridarolli [b], Marianne Odlyha [b], Laurent Bozec [b], Marta Oriola [c], Gema Campo Francés [c], Michael Persson [a,d], Krister Holmberg [a], Romain Bordes [a,*]

[a] Department of Chemistry and Chemical Engineering, Applied Surface Chemistry, Chalmers University of Technology, 412 96 Gothenburg, Sweden

[b] Department of Biological Sciences, Birkbeck College, University of London, Malet Street, Bloomsbury, London WC1E 7HX, United Kingdom

[c] Department of Arts and Conservation, Faculty of Fine Arts, University of Barcelona, C/Pau Gargallo, 4, 08028 Barcelona, Spain

[d] AkzoNobel Pulp and Performance Chemicals AB, Sweden

[1] Present address: Swerea IVF AB, Box 104, SE-431 22 Mölndal, Sweden

[2] Present address: Department of Chemistry and Molecular Biology, University of Gothenburg, Göteborg, Sweden

* Corresponding authors: oleksandr.nechyporchuk@swerea.se (O.N.); bordes@chalmers.se (R.B.)

Graphical abstract

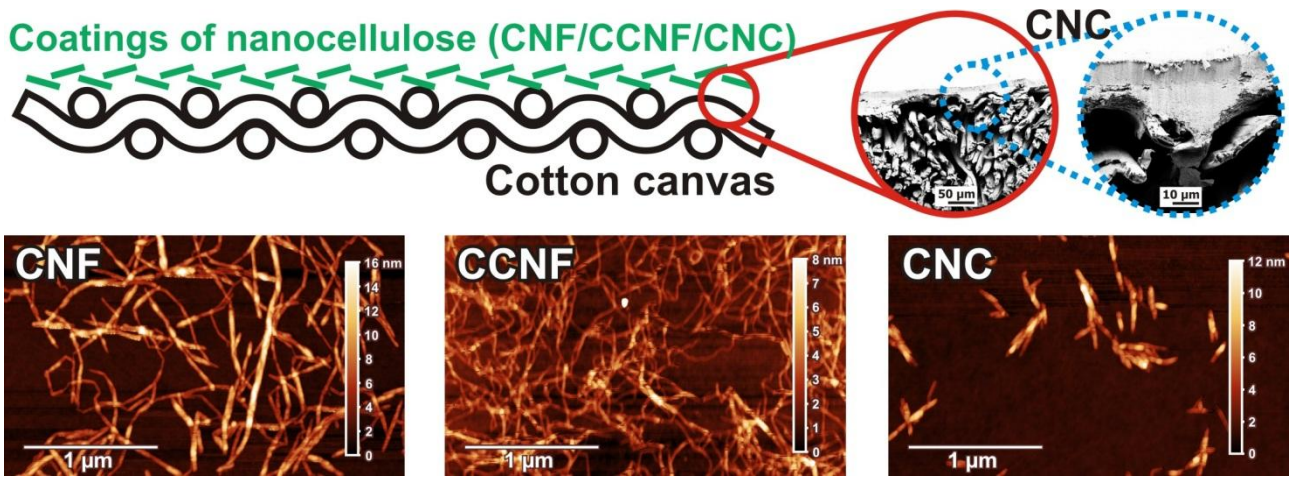

Abstract

Nanocellulose has been recently proposed as a novel consolidant for historical papers. Its use for painting canvas consolidation, however, remains unexplored. Here, we show for the first time how different nanocelluloses, namely mechanically isolated cellulose nanofibrils (CNF), carboxymethylated cellulose nanofibrils (CCNF) and cellulose nanocrystals (CNC), act as a bio-based alternative to synthetic resins and other conventional canvas consolidants. Importantly, we demonstrate that compared to some traditional consolidants, all tested nanocelluloses provided reinforcement in the proper elongation regime. CCNF showed the best consolidation per added weight, however, it had to be handled at the lowest solids content compared to other nanocelluloses, exposing canvases to larger water volumes. CNC reinforced the least per added weight but could be used in more concentrated suspensions, giving the strongest consolidation after an equivalent number of coatings. CNF performed between CNC and CCNF. All nanocelluloses showed better consolidation than lining with Beva 371 and linen canvas.

Keywords

Conservation, restoration, consolidation, easel paintings, cellulose nanofibrils (CNF), cellulose nanocrystals (CNC)

1 Introduction

Painting canvases made from natural fibers (*e.g.*, linen, hemp, cotton or jute), used by artists as painting support, age over time. The ageing occurs due to temperature and humidity variations, and hence the dimensional changes of the painting mounted on a stretcher (Hedley, 1988; Hendrickx, Desmarais, Weder, Ferreira, & Derome, 2016), as well as chemical processes caused by acidity, originating from primers, paints, glues and absorption of acidic gases from the environment (Ryder, 1986; Oriola et al., 2014). The ageing results in canvas degradation, particularly the reduction of its

mechanical properties, which may lead to cracking of the paint layer as well as accidental tears of the canvas, resulting in irreversible damage of the painting.

In order to consolidate degraded canvases two options can be used: (i) consolidating the original canvas with an adhesive and (ii) lining of the original canvas with a new one, i.e. gluing the new canvas over the old one (Stoner & Rushfield, 2012). In both strategies, the damaged substrate on the back side of the painting is treated by an adhesive, which may be natural, such as animal glue and glue-paste, or synthetic, such as acrylic (Plexisol PB550, Paraloid B72 or Plextol B500) or complex wax-resin formulations (Beva 371) (Berger, 1972; Ackroyd, 2002; Ploeger et al., 2014). Generally, water-based adhesives are less favorable due to the hygroscopic character of the cellulosic canvas. Swelling and shrinkage of the canvas occur as a response to interactions with water, resulting in dimensional changes of the painting. The choice of proper material for canvas restoration is a major concern for conservators and the ideal properties of such materials are still under debate. One of the opinions with respect to lining and lining adhesive is to provide the painting with a stiffer support to which the mechanical stress is transferred (Ackroyd, 2002; Young, 1999; Berger & Russell, 1988). This reduces the load accumulated in the paint layer and minimizes the future degradation of the painting. At the same time, it is important to allow elongation of the lining from 0.3 to 3.0%, which is the elongation range to which paintings are exposed when mounted on a stretcher. It varies depending on the type of canvas, warp or weft direction, the pigments used and the age of the painting (Mecklenburg, 1982, 2005; Mecklenburg & Fuster Lopez, 2008).

Lining has traditionally been used for canvas restoration. However, with the growing interest in methods that provide minimal intervention of the painting, treatments other than lining have become popular in the last decades (Ackroyd, Phenix, & Villers, 2002; Villers, 2004). The alternative treatments become favorable mainly due to the issues of reversibility, aesthetic concerns, excess of added new materials and no access to the original canvas with a lining. Another reason is that some of the widely used synthetic adhesives, such as Beva 371, are questionable from health and environmental point of view due to their toxicity (Bianco et al., 2015). Some synthetic adhesives, such as poly(vinyl acetate), promote canvas degradation due to acidic products formed during their own degradation (Chelazzi et al., 2014) and are therefore no longer used. These concerns have resulted in an increased use of natural polymers, such as animal or fish glue, for canvas reinforcement (Ackroyd, 2002).

The degraded canvas generally possesses defects at different length scales, *e.g.*, fiber cracks on the micrometer scale and depolymerization of cellulose chains on the nanometer scale. In order to restore the mechanical properties of the original canvas, these issues should be tackled (Kolman, Nechyporchuk, Persson, Holmberg, & Bordes, 2017). In addition to the physico-chemical properties of the canvas fibers, the morphology of woven fabric has a strong influence on the

mechanical properties (Young & Jardine, 2012). Taking into consideration that the paint layer, as well as the ground or size, are much stiffer than the canvas, the conservation treatment may aim at an efficient reinforcement for the canvas, rather than at restoration of the original properties, including high stretchability and flexibility, as these properties have been lost with the application of the different preparative layers. In parallel to the mechanical reinforcement, deacidification of the canvas needs to be carried out in order to arrest further degradation (Giorgi, Dei, Ceccato, Schettino, & Baglioni, 2002).

In the recent development of cellulose-based materials, nanocellulose has emerged and generated a strong interest, often due to its unique mechanical properties. Nanocellulose can be divided into three main categories: (i) cellulose nanocrystals (CNC), also referred to as nanocrystalline cellulose (NCC) or cellulose whiskers (Habibi, Lucia, & Rojas, 2010; Rånby, 1949); (ii) cellulose nanofibrils (CNF), also known as nanofibrillated cellulose (NFC) or microfibrillated cellulose (MFC) (Turbak, Snyder, & Sandberg, 1983; Nechyporchuk, Belgacem, & Bras, 2016), and (iii) bacterial nanocellulose. CNC and CNF are much more common, since they are produced by delamination of cellulose microscopic fibers (generally, from wood) into nanomaterial (top–down process), whereas bacterial nanocellulose is generated by a buildup (bottom–up process) from low molecular weight sugars by bacteria (Nechyporchuk, Belgacem, & Bras, 2016). Bacterial cellulose is produced in the form of biofilms (pellicles) of determined dimensions that contain interconnected nanofibrils (Klemm, Heublein, Fink, & Bohn, 2005), whereas CNC and CNF are separate nanoparticles, thus their deposition is not limited by the physical dimensions of the artifacts. In order to deposit bacterial nanocellulose from suspensions, post-fibrillation should be performed.

The different types of nanocellulose present appealing features for the purpose of canvas consolidation: they have high strength and form transparent/translucent and lightweight films. Their non-toxic character and non-abrasiveness for processing equipment, as well as renewable and biodegradable character, are additional features of interest for the field. Nanocellulose also has a large surface area and there are well-developed methods for its surface modification (Habibi et al., 2010; Moon, Martini, Nairn, Simonsen, & Youngblood, 2011; Nechyporchuk, Belgacem, & Bras, 2016). Reinforcing a cellulosic canvas with a material of similar nature can be beneficial for future preservation of canvas paintings.

The interest in using nanocellulose for restauration of cellulosic materials has been increasing lately. Nanocellulose has recently been employed for consolidation of historical papers (Santos et al., 2015; Dreyfuss-Deseigne, 2017; Völkel, Ahn, Hähner, Gindl-Altmutter, & Potthast, 2017). Bacterial nanocellulose has been also reported for reinforcement of historical silk fabrics (Wu, Li, Fang, & Tong, 2012). To the best of our knowledge, the use of nanocellulose for consolidation of painting canvases remains unexplored.

In this work, different types of nanocellulose, namely mechanically isolated cellulose nanofibrils (CNF), carboxymethylated cellulose nanofibrils (CCNF) and cellulose nanocrystals (CNC), were tested and compared in terms of structural reinforcement of degraded canvases. The mechanical properties of newly prepared and real paintings were first studied to determine the elongation regime where canvas consolidation should act. Then, model aged canvases were treated with different nanocellulose-based formulations to investigate their film-forming properties on canvases and their response to static and periodic uniaxial stress at different relative humidity values. The reinforcing effect of the nanocelluloses was also compared with that obtained with different traditional consolidants.

2 Materials and methods

2.1 Materials

CNF in the form of an aqueous suspension was kindly provided by Stora Enso AB (Sweden). The CNF was produced from softwood pulp (*ca.* 75% of pine and 25% of spruce, containing 85% of cellulose, 15% of hemicellulose, and traces of lignin, as determined by the supplier). CCNF, also in the form of an aqueous suspension, was kindly provided by RISE Bioeconomy (Sweden). The CCNF was produced from a softwood sulphite dissolving pulp (Domsjö Dissolving plus, Domsjö Fabriker AB, Sweden) by carboxymethylation, as described previously (Wågberg et al., 2008), followed by mechanical fibrillation. CNC in powder form was purchased from CelluForce (Canada). It was produced from bleached kraft pulp by sulfuric acid hydrolysis. Charge densities of –20.7 ± 0.6, –151 ± 2 and –259 ± 4 µeq/g at pH 5.2 were measured for CNF, CCNF and CNC, respectively, using a particle charge detector PCD-02 (Mütek Analytic GmbH, Germany), titrated using poly(diallyldimethylammonium chloride). Tetrabutylammonium hydroxide (TBAOH) as a 20 wt % aqueous solution and calcium chloride (≥96.0%) were purchased from Sigma-Aldrich, Sweden.

Cotton canvas with a basis weight of 417 ± 3 g/m^2 and a plain weave was obtained from Barna Art (Barcelona, Spain). Dry animal glue from Lienzos Levante (Spain) was used as a sizing agent or as a consolidant. Lefranc & Bourgeois® Gesso acrylic-based medium with titanium dioxide, calcium carbonate and potassium hydroxide was used as a primer. Titanium White Rutile acrylic paint from Vallejo® (Acrylic artist colour. Extra fine quality acrylic, ref 303), Cadmium Red Medium acrylic paint from Vallejo® (Acrylic artist color. Extra fine quality acrylic, ref 805) and Liquitex® professional gloss varnish were used to prepare the painted canvas samples. A cellulose ether (hydroxypropyl cellulose) Klucel® G, an acrylic resin Paraloid® B72 and Beva Original Formula® 371 Film lining were products from CTS Spain.

2.2 Samples of painted canvas and real paintings

The cotton canvas was washed by soaking overnight in a water bath. It was then dried and mounted onto a stretcher. One layer of animal glue at 9.6 w/v% and *ca.* 60 °C was applied on the canvas with a brush. Then, two layers of primer were applied with a plastic serigraphy squeegee in cross directions. After that, two thin paint layers were applied using a soft foam roller in cross directions. Finally, one varnish layer was applied using a flat soft brush. All the layers were let dry several weeks before applying the next one.

The real painting used in this study had an acrylic paint layer on a modern commercially prepared cotton canvas that was about 15 years old. It had very thin and flexible preparation and paint layers on a thin canvas too.

2.3 Canvas accelerated ageing

A model of the degraded canvas was prepared as reported previously (Nechyporchuk, Kolman, et al., 2017). In brief, the method consists of treating pristine cotton canvas (70 × 80 mm) with a mixture of 200 mL hydrogen peroxide solution (35 wt%) and 10 mL sulfuric acid during 72 hours at 40 °C. As a result, the cellulose degree of polymerization (DP) decreased from *ca.* 6250 to *ca.* 450 and the breaking force for a 10 mm wide canvas stripe was reduced from 176 ± 8 N to 42 ± 4 N (Nechyporchuk, Kolman, et al., 2017). The canvas basis weight was reduced to 374 ± 3 g/m^2.

2.4 Application of nanocellulose consolidation treatments

In order to achieve similar viscosity, aqueous suspensions of CNF, CCNF and CNC were prepared by dilution with deionized water at concentrations of 1.00, 0.25 and 3.00 wt.%, respectively, and then homogenized using a Heidolph DIAX 900 (Heidolph Instruments, Germany) equipped with a 10 F shaft at power 2 (around 11,600 rpm). These suspensions were homogeneously spread on the surface of the aged cotton canvas samples (70 × 80 mm) using a plastic serigraphy squeegee. The coatings were deposited in 1–3 passes with an interval of 20 min to allow some water to evaporate. Table 1 shows the increase of the canvas basis weight after coating, measured by gravimetry. After drying, one batch of CCNF canvas samples, with different amount of deposited nanocellulose, was treated with a 0.5 M $CaCl_2$ aqueous solution (ca. 2 g of solution per m^2) to cross-link the nanofibrils (Dong, Snyder, Williams, & Andzelm, 2013), which was applied by spraying with a Cotech Airbrush Compressor AS18B (Clas Ohlson AB, Sweden) at a pressure of 2 bar. One batch of samples was prepared by mixing CCNF suspensions with TBAOH (5/1 wt/wt dry) to reduce the hydrophilicity of the cellulose (Shimizu, Saito, Fukuzumi, & Isogai, 2014).

Table 1 List of treatments used for aged canvas consolidation and the basis weight uptake after the coating.

Sample name	Description	Basis weight uptake (%) with number of coatings		
		1	2	3
CNF	Canvas coated with cellulose nanofibril suspension at 1 wt.%	2.5	5.0	7.2
CCNF	Canvas coated with carboxymethylated cellulose nanofibril suspension at 0.25 wt.%	0.6	1.2	1.8
CNC	Canvas coated with cellulose nanocrystal suspension at 3 wt.%	7.4	14.8	22.2

2.5 Application of conventional consolidants

Three different adhesives, animal glue, Klucel G and Paraloid B72, which have been traditionally used to consolidate painting canvases, were applied on the aged cotton canvas as shown in Table 2. A lining of the aged canvas using a Beva 371 film and a new linen canvas was also performed. The canvas was fixed on a flat rigid surface along the borders to avoid shrinkage during the treatment. When brushing, a flat 4 cm wide brush was used. When using an airbrush, samples were set in an upright position and applications were performed from a distance of 10 cm to cover the canvas homogeneously in horizontal and vertical directions. A limited amount of consolidant was applied during spraying to avoid flooding the canvas, which is important in order to avoid canvas shrinkage. Coatings were left to dry for 5–10 minutes between applications. Profi-AirBrush Compact II airbrush was used, with a 0.3 mm needle, consolidant gravity feed and 2.5 bar pressure.

Table 2 List of traditional consolidants applied on the aged canvases

Sample name	Concentration and solvent	Application system and number of coatings
Animal Glue	5 w/v% in water	Brush, 1 coating, soaking the canvas
Klucel® G	1 w/v% in ethanol	Airbrush, 4 coatings without soaking the canvas
Paraloid® B72	5 w/v% in acetone	Airbrush, 1 coating without soaking the canvas
		Brush, 1 coating, soaking the canvas
Beva Original Formula® 371 Film (lining)	Film	Lining onto a new linen canvas. Beva film first attached to the lining canvas, then to the cotton sample with a hot spatula at 65ºC

2.6 Tensile testing

Mechanical testing was carried out according to the ASTM D5034 – 09 method ("ASTM D5034 − 09 (2013) Standard Test Method for Breaking Strength and Elongation of Textile Fabrics (Grab Test)," 2013) with slight deviations. The measurements were performed using Instron 5565A (Norwood, MA, USA) equipped with a static load cell of 100 or 5000 N and pneumatic clamps operated at a pressure of 5 bar. Rectangular specimens with a length of 70 mm and a width of 10 mm were cut parallel to the warp or the weft direction along the threads. The samples were

conditioned at least 12 h before the measurements at a relative humidity (RH) of 60% and a temperature of 23 °C. Sandpaper was used between the canvas sample and the clamps (with the grains facing the canvas) to avoid slippage. The measurements were carried out at a constant extension rate of 300 mm/min and a gauge length of 20 mm. The force was measured as a function of elongation and then expressed in Newtons per meter of canvas length (Berger & Russell, 1988) . Seven measurements were performed for each specimen and the average values were then calculated. A digital video camera operating at 30 frames per second was used for video recording during the tensile testing of the samples of painted canvas and real painting in order to detect the point where the cracking became visible.

2.7 Atomic force microscopy (AFM)

AFM was performed in tapping mode using NTEGRA Prima equipped with a NSG01 cantilever (NT-MDT, Russia) to examine the morphology of the nanocellulose samples. For sample preparation, the CNF/CCNF and the CNC suspensions were diluted to a concentration of 10^{-2} and 10^{-3} wt.%, respectively, and a droplet of each suspension was placed on a freshly polished silicon wafer substrate and dried. The AFM height images were then processed with the Gwyddion software. The nanoparticle diameter was determined from the height profiles of AFM height images as an average of 100 measurements.

2.8 Scanning electron microscopy (SEM)

The cross-section of the coated canvases was analyzed using Leo Ultra 55 field emission gun (FEG) SEM (Carl Zeiss SMT GmbH, Germany). The SEM was operated at an acceleration voltage of 3 kV. The canvas cross-section was prepared by clear cut with a new razor blade punched with a hammer. The samples were mounted onto stubs and sputtered with a gold layer of *ca.* 10 nm using a Sputter Coater S150B (Edwards, UK).

2.9 Controlled relative humidity dynamic mechanical analysis (DMA-RH)

Dynamic mechanical analysis was carried out using a Tritec 2000 B (Lacerta Technology Ltd., UK) equipped with a humidity controller. The samples were cut in warp direction with a width of 10 threads and a gauge length of 5 mm. The measurements were carried out at a frequency of 1 Hz, an amplitude of 0.1% of strain and a temperature of 25 °C. The samples were subjected to ramps in the region of 20–60 %RH at a rate of 4 %RH/min with an equilibration at each RH of 30 min. Three RH cycles (20–60%RH) were performed for each sample.

3 Results and Discussion

3.1 Mechanical properties of canvas paintings

In order to provide a rational reinforcement of the degraded canvases, it was necessary to determine the elongation regime where the reinforcement should be provided, *i.e.*, to specify

whether the initial stretchable character of the canvas should be reproduced or if the consolidation treatment should stiffen the canvas. New cotton canvas was coated with prime, paint and varnish, and was examined after each layer deposition in both warp and weft directions using tensile testing.

The force-elongation curves both in warp and weft directions are shown in Fig. 1a and b, respectively. The measurements revealed an increase of the breaking force and a slight reduction of elongation at break in both directions when the canvas was primed. The values went from 17.6 ± 0.8 kN/m to 24.0 ± 1.4 kN/m for the breaking force and from 52.7 ± 1.1% to 48.9 ± 2.7% for the elongation at break in warp direction. A sharp increase of the slope of the curve in low elongation regime after priming indicates its stiffening effect. Taking into account an increase of canvas thickness from 0.814 mm to 0.948 mm as a result of the priming, and applying the reduction factor of 25% for the canvas cross-section (area of the threads parallel to the force direction) (Mecklenburg, McCormick-Goodhart, & Tumosa, 1994), the Young's modulus in the linear domain of elongation (<2%) in the warp direction was quantified as 17.6 ± 0.8 MPa and 356.0 ± 18.0 MPa for the original and the primed canvas, respectively. The subsequent application of paint and varnish, which were both much thinner than the prime layer, did not significantly affect the mechanical behavior.

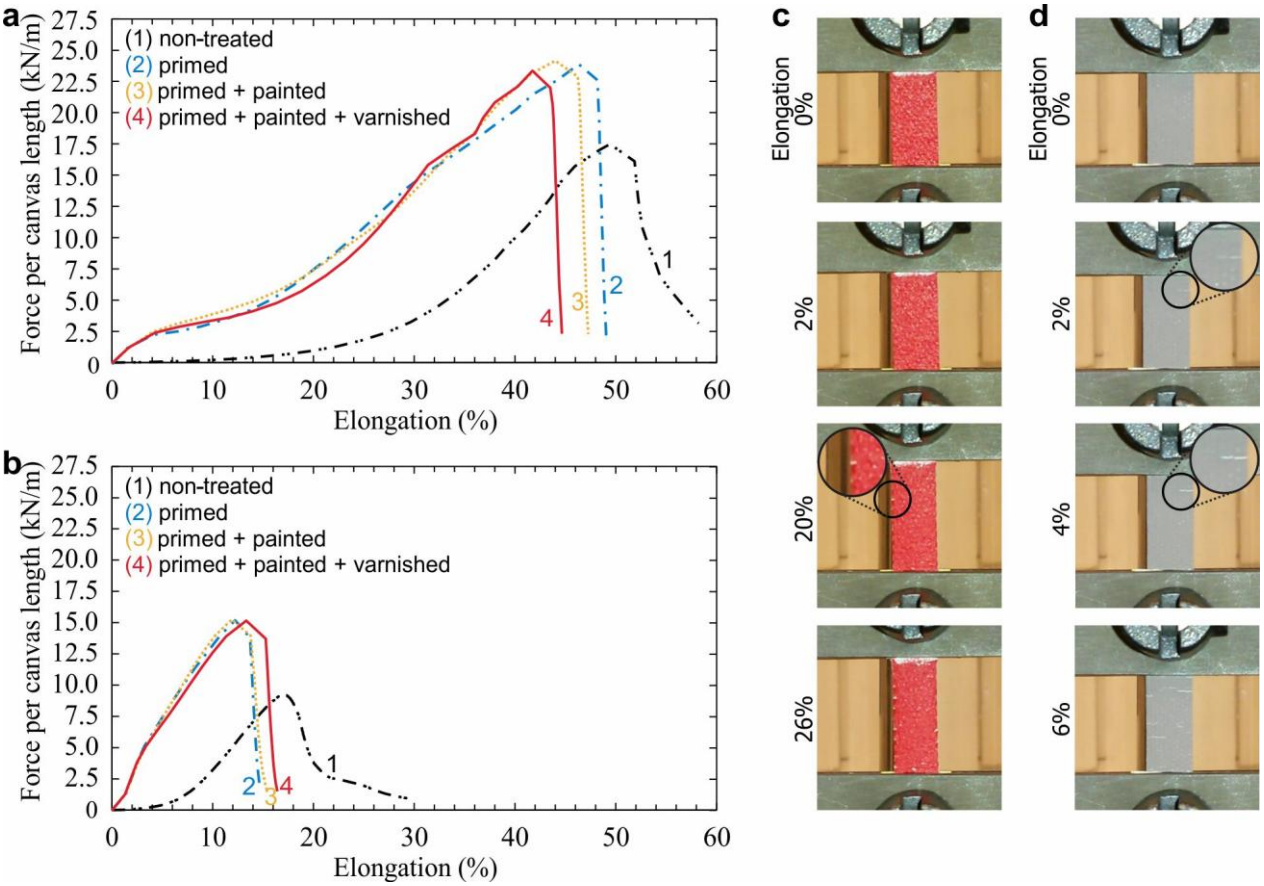

Fig. 1. Mechanical properties of new cotton canvas treated with prime, paint and varnish layers, measured in (**a**) warp and (**b**) weft directions. Images of the primed and painted new canvas (**c**) and real painting (**d**), both captured during tensile testing at various elongations, measured in warp direction. The circles in **c** and **d** show crack propagation.

The linear region of deformation of the painted canvases was found to be quite short (<2% elongation). Outside this region the deformation is known to be irreversible (Stachurski, 1997) and the paint layer is likely to deteriorate. Therefore, the consolidation treatment should provide substantial reinforcement in this region to prevent paint cracking. The samples that were primed and painted were first examined visually to detect possible cracks. On Fig. 1c, which relates to a freshly made painting, the propagation of cracks became noticeable only at *ca.* 20% elongation. In comparison, for the real painting samples shown in Fig. 1d, the paint layer started to crack already at 2% elongation. The increased brittleness of aged paintings is a known phenomenon and is due to chemical changes, such as gradually increasing degree of crosslinking and loss of plasticizer (Michalski, 1991). Prevention of this process is crucial; otherwise, it will eventually lead to flaking and to the deterioration of the paint layer. Such a low elongation regime for paint cracking suggested that the consolidation treatment should provide a stiff support at low elongation in order to prevent paint cracking, which was also suggested previously (Berger & Russell, 1988).

3.2 Consolidation of aged canvas with nanocellulose: morphological characterization

The reinforcement potential of the different nanocellulose samples, *viz.*, CNF, CCNF and CNC, was analyzed in this study as an alternative to conventional consolidation practices. The nanocellulose formulations were examined on a model of degraded cotton canvas developed previously (Nechyporchuk, Kolman, et al., 2017). The morphology of these nanocelluloses is shown in Fig. 2a–c. CNF (Fig. 2a) had a thickness of 7.0 ± 2.8 nm and a length of several micrometers. CNC (Fig. 2c) had similar diameter, 7.5 ± 2.8 nm, but was smaller in length, *ca.* 0.5 μm. Finally, CCNF (Fig. 2b) was much thinner compared to the others, 2.4 ± 0.9 nm, and had a length of several micrometers.

Simplified surface chemical structures of CNF, CCNF and CNC are shown in Fig. 2d, e and f, respectively. These nanocellulose samples were extracted from wood using different processing routes, including surface functionalization for CCNF and CNC. Carboxymethyl and sulfate ester groups resulted in the presence of negative charges on the surface at basic and neutral pH (charge densities are shown in the Materials and Methods section). This introduced repulsive interactions between the nanofibers and gave better dispersibility, which may enhance the penetration into the canvas. The dimensional and surface charge differences among the nanocelluloses may influence the film-forming properties on canvases and the final mechanical properties of the coated canvases. Additionally, CCNF and CNC can exhibit acidic character, as the pKa of the functional groups is below 7, which should be considered for achieving long-term stability of the consolidation treatment. However, when deacidification of the canvas is performed and a certain alkaline reserve

is present (Giorgi et al., 2002), its buffering activity may avoid the acidity issue. This question remains beyond the present work and requires further investigation.

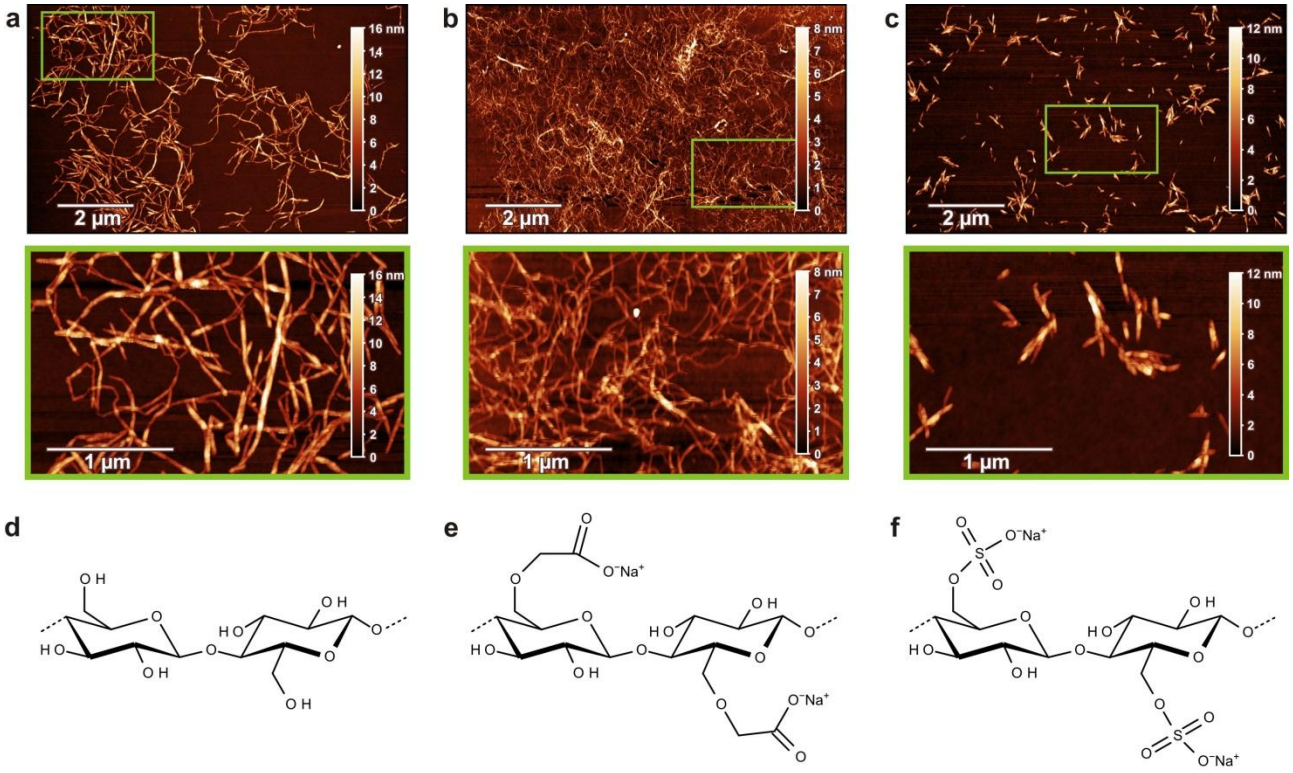

Fig. 2. Atomic force microscopy images (**a**, **b**, **c**) and the corresponding simplified surface chemistries (**d**, **e**, **f**) of: (**a**, **d**) mechanically isolated cellulose nanofibrils (CNF); (**b**, **e**) carboxymethylated cellulose nanofibrils (CCNF) and (**c**, **f**) cellulose nanocrystals (CNC). The color gradient bars shown in the AFM images represent the height scale, also referred to as the thickness.

Fig. 3a, b and c show SEM images of cross-sections for the canvas samples coated with 3 layers of CNF, CCNF and CNC, respectively. From the upper SEM images, the nanocellulose coatings are barely seen. Instead, the canvas structure, consisting of microscopic fibers, is clearly visible. It is seen that none of the nanocelluloses penetrated much into the canvas bulk, instead, forming a film on the canvas surface. It is interesting that this was the case also for CNC, which, as discussed above, consists of short nanoparticles that unlike CNF do not form highly entangled flocs (Nechyporchuk, Pignon, & Belgacem, 2015). One may anticipate large flocs present in CNF to be trapped by the canvas fibers and, therefore, not penetrate much into the porous material. However, it is obvious that a non-flocculated suspensions of charged CCNF and CNC also resist penetration. Similar film-forming properties have been observed previously when coating textiles with CNF (Nechyporchuk, Yu, Nierstrasz, & Bordes, 2017).

We assume that the poor penetration is related to fast water absorption by canvas fibers from the nanocellulose suspensions, which leads to increased viscosity of the suspensions and arrested flow into the canvas depth. Application of further coating layers leads to a better-developed continuous

film on the canvas surface. Such good film-forming properties on the canvas surface without noticeable penetration have a good potential to result in reversible consolidation treatment, which can be further removed from the surface, if necessary.

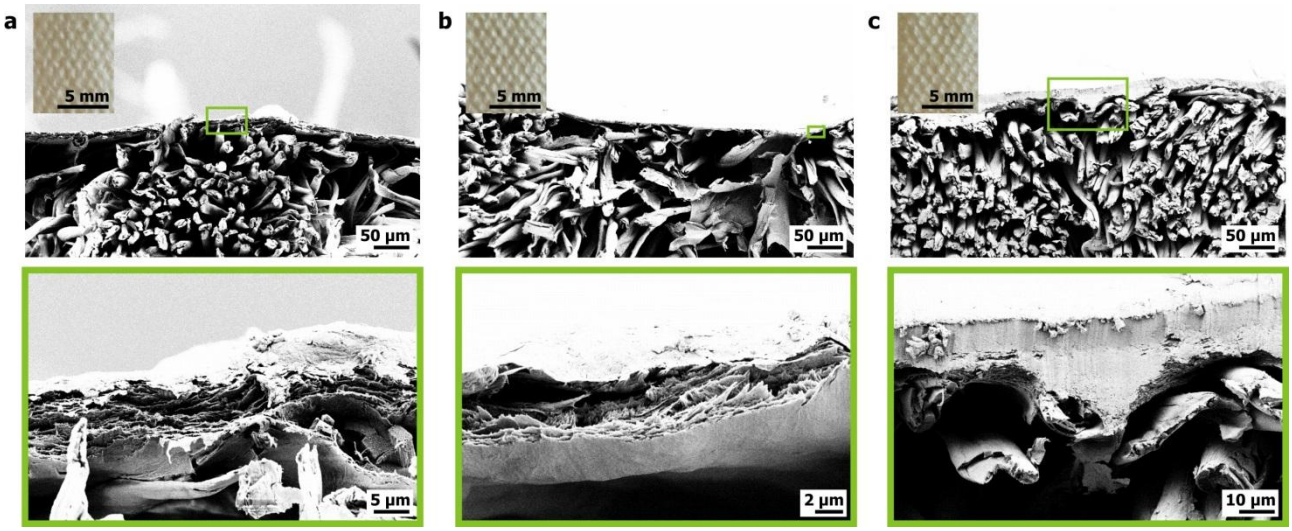

Fig. 3. Scanning electron microscopy images of aged cotton canvases coated 3 times with: (**a**) CNF; (**b**) CCNF and (**c**) CNC, with optical microscopy images as insets (left top).

It was also observed that CNF and CCNF formed highly porous films with lamellar self-assembled structure (see Fig. 3a, b). Similar structures have been previously reported for self-standing CNF films prepared by different methods (Henriksson, Berglund, Isaksson, Lindström, & Nishino, 2008; Li et al., 2016) and for CNF coatings on fabrics (Nechyporchuk, Yu, Nierstrasz, & Bordes, 2017). CNC tended to form more dense structures (see Fig. 3c) due to better packing capacity of rod-like nanoparticles, compared to the flexible nanofibrils. Additionally, the insets (top left) in Fig. 3a, b and c show that such nanocellulose films do not distinctly change the visual appearance of the canvases, which is in line with the minimal intervention principle of canvas restoration (Ackroyd et al., 2002), especially compared to lining with a new canvas.

3.3 Mechanical properties of the consolidated aged canvased

Fig. 4 shows force-elongation curves for model aged canvases coated with different nanocellulose-based formulations measured in warp direction. Mechanical properties of the painted pristine canvas are also given as reference. The canvases with one, two or three coatings with a given consolidation formulation are shown, as well as the bare degraded canvas. The curve representing an average of seven measurements for each sample is plotted. The mechanical properties in low elongation regime are the most important here, as discussed previously, and are shown in insets. However, we also present the whole curves in order to compare the performance of

nanocellulose treatments further with conventional consolidants, since some of them provide more distinct features in the whole elongation range.

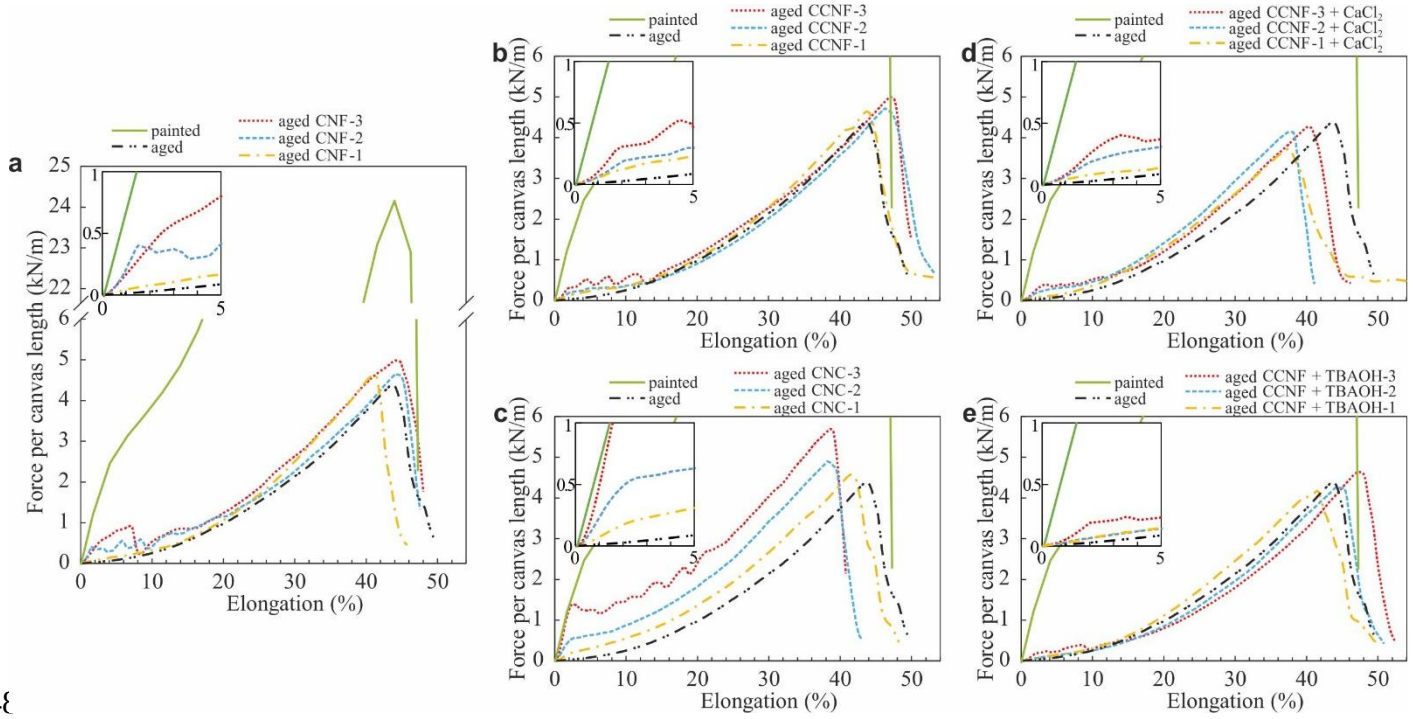

Fig. 4. Mechanical properties of the aged canvases coated with different number of coatings of: (**a**) CNF, (**b**) CCNF, (**c**) CNC, (**d**) CCNF + $CaCl_2$ and (**e**) CCNF + TBAOH. The curves for painted new canvas are also shown.

As can be seen from Fig. 4a, the slope of the tensile curves enhanced drastically in the low elongation region (< 5%) by applying CNF, see Fig. 4a, indicating the increase of stiffness. Since the coatings did not much influence the canvas thickness, this led to an increase of Young's modulus. The larger the number of coatings on the canvas, the larger the increase of the modulus. The use of CNF gave an increased force over the entire elongation range and increased the breaking force. In the elongation range of 5–10%, some fluctuations of the force were observed, which can be attributed to cracking of the nanocellulose coating. In this case, the periodic decrease of the measured force occurred due to inertia created after breakage of the coating.

The inset in Fig. 4a demonstrates better the low elongation regime of the canvas coated with CNF. The CNF consolidation with 3 layers exhibits linear (reversible) deformation up to ca. 500 N/m at an elongation of up to 3%, which exceeds the maximum sustainable tension of 200–300 N/m above which an average painting canvas is torn (Berger & Russell, 1990; Iaccarino Idelson, 2009; Roche, 1993). Even though the curve had a lower slope than a painted new canvas, the improved stiffness compared with that of the aged canvas was significant. The coating with 2 CNF layers can be considered as an acceptable level of consolidation as well. Such stiffening effect is well in line with previous studies (Völkel et al., 2017; Nechyporchuk, Yu, et al., 2017).

The use of CCNF resulted in a smaller increase of the stiffness, as compared to CNF. This occurred since a lower concentration of nanocellulose was used in the case of CCNF suspension, resulting in lower dry weight increase of the coating (see Table 1). A lower concentration was used because of the higher nanofibril aspect ratio of CCNF, which led to more viscous gels at equivalent concentrations (Nechyporchuk, Belgacem, & Pignon, 2016). With CCNF as coating material, the canvas exhibited not only a higher breaking force compared to neat canvas, it gave higher elongation at break as well, which is probably also related to the higher nanofibril aspect ratio. Three coatings with CCNF, which in terms of mass gain is close to one coating with CNF, yielded a higher curve slope than the canvas coated with one layer of CNF, suggesting that a higher level of reinforcement can be achieved with the same deposited dry weight of coating.

CNC coatings provided the lowest level of reinforcement normalized by the deposited weight, which can be explained by the fact that they possess the lowest aspect ratio. On the other hand, the possibility of coating with a suspension of higher concentration resulted in better reinforcement compared to the others when three coating layers were deposited. When using CNC, both Young's modulus and the breaking force increased, while the elongation at break was reduced. The mechanical behavior of the coated canvas with 3 layers of CNC in the low elongation regime (up to 3%) matched perfectly the behavior of newly painted canvas, thus suggesting that such level of reinforcement can well support the paint layer, see inset in Fig. 4c. The coating with 2 layers of CNC also provided an acceptable level of reinforcement.

Attempts to improve the mechanical properties of CCNF by ionic cross-linking or to reduce its sensitivity to water by hydrophobization with TBAOH did not give major improvements, as shown in Fig. 4d and e.

The nanocellulose suspensions used are all aqueous, which means that each application introduces water into the canvas, which is then evaporated. These events should be minimized in order to prevent dimensional variations of the canvas due to swelling and shrinkage. Therefore, the canvas consolidation treatment will be a compromise between the highest possible reinforcement, the lowest mass uptake (which are both best provided by CCNF) and the lowest water content in the suspension (best provided by CNC). CNF is in-between CCNF and CNC in these regards. The suspensions were manipulated in this work at concentrations that allowed them to be sprayed on the canvas using an airbrush. This may reduce the amount of water exposed to the canvas due to enhanced evaporation during spraying. No distinct difference in the extent of nanocellulose penetration into the canvas was observed when comparing spraying and application using a brush.

The newly developed consolidation treatments can be seen as an alternative to the conventional ones. Therefore, the mechanical properties of the model aged cotton canvases treated with some traditional restoration materials were studied and compared with the values obtained with the

nanocellulose coatings. Fig. 5a shows that Klucel G (hydroxypropyl cellulose), a popular leather and paper consolidant, reduced slightly the elongation at break without affecting much Young's modulus and the breaking force. Therefore, at that deposited quantity, it did not provide proper canvas reinforcement. Similar behavior was observed for sprayed Paraloid B-72 (acrylic resin). When the same formulation was applied by brush, a distinct improvement of the mechanical properties was observed, however. There was an increase in both Young's modulus and the breaking force. Finally, the use of rabbit skin glue resulted in a strong enhancement of both stiffness and strength.

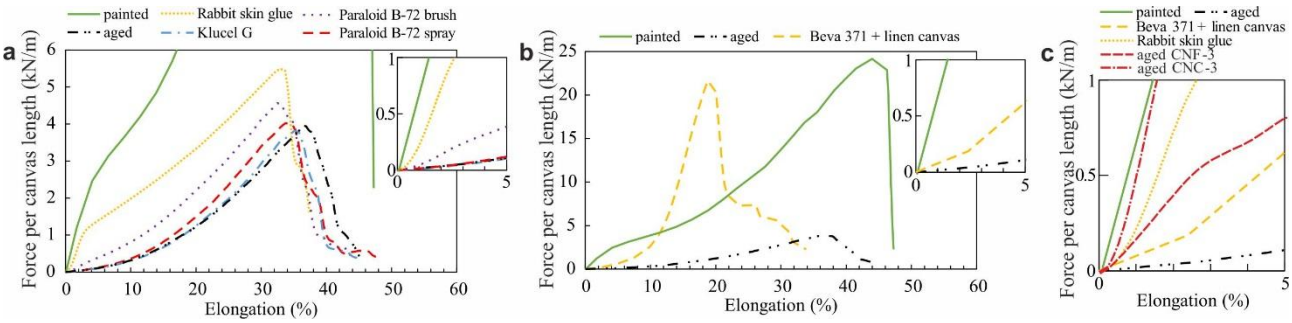

Fig. 5. Mechanical properties of aged canvases after various consolidation treatments

Fig. 5b shows the mechanical properties of the aged canvas coated with Beva Original Formula® 371 Film and lined with a linen canvas. The strength of the consolidated canvas almost reached the value of the newly painted canvas. However, the stiffness was not increased much in the low elongation region; thus, the treatment did not provide a stiff support for the paint. In the range usually used to stretch paintings (0 N/m to 300 N/m and 0% to 3% elongation) among all the materials shown in Fig. 5 only the animal glue reinforced the canvas in a proper way. On the other hand, deposition of animal glue is known to cause strong contraction of the canvas upon drying (Ackroyd, 2002). Fig. 5c provides direct comparison of the best performing traditional consolidants with nanocellulose coatings (3 layers) in low elongation region. Compared to the conventional consolidants, CNC showed the highest level of consolidation. Both CNC and CNF provided better reinforcement than conventional lining with Beva Original Formula® 371 Film and linen canvas.

3.4 Influence of relative humidity (RH) variations on the mechanical stability of the consolidated canvases

In order to confirm the suitability of nanocelluloses as an alternative to traditional consolidants, it is important to assess the influence of variations in RH on the mechanical properties of the treated models of degraded canvas. DMA-RH has been used previously to evaluate effects of environmental conditions and preventive conservation treatment on painting canvases (Foster,

Odlyha, & Hackney, 1997). Variations in RH can influence the dimensional stability of the canvas and a nanocellulose layer responding too strongly to environmental changes would be detrimental. Fig. 6a shows the variation of storage modulus (E') between two relative humidity levels measured with DMA-RH on the 2nd cycle. The humidification and dehumidification profiles are shown separately in Fig. 6b and c, respectively. It can be seen that the response to RH variations for coated and uncoated samples was similar: all the samples exhibited higher stiffness at low RH (20%) and lower stiffness at high RH (60%). This effect can be explained by a plasticizing action of water molecules on the cellulosic chains. An increased water content will lead to reduced intermolecular cellulose interactions through hydrogen bonding.

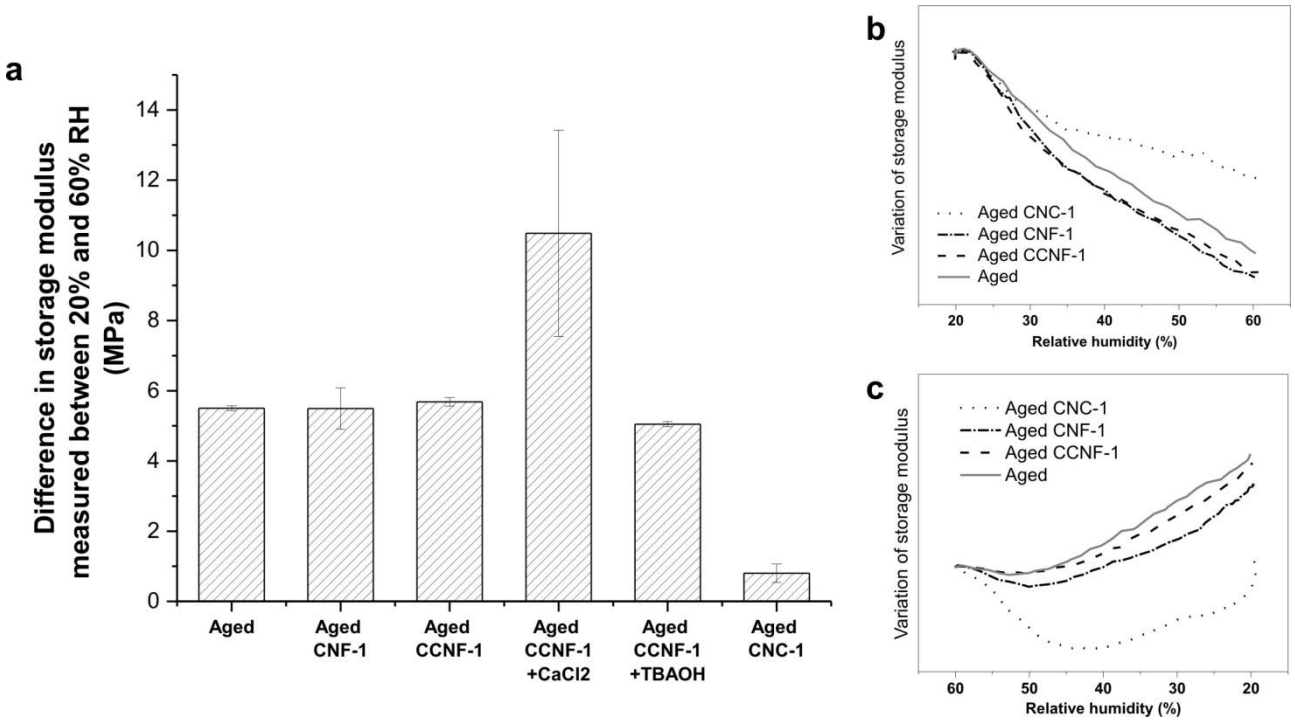

Fig. 6. Variation of the storage modulus of consolidated aged canvases applying different relative humidity levels (**a**), including humidification (**b**) and dehumidification (**c**) profiles.

The variation of E' was similar for the aged canvas and the one coated with CNF and CCNF (Fig. 6a). The smallest differences in stiffness at the RH plateaus were observed for CNC despite this material having highly hydrophilic sulfate groups (see Fig. 2f) on the surface. This may be explained by the higher density of the CNC coatings as compared to the coatings with CNF and CCNF, as shown previously in Fig. 3. The use of calcium chloride for ionic cross-linking of the CCNF coating resulted in a much enhanced variation of E'. Most likely, this is due to the excess of salt that was introduced. Free salt in the material will make it more responsive towards moisture changes. These results demonstrate the difficulties of such a cross-linking approach. Finally, the use

of TBAOH did not much influence the stiffness variations, although one may expect that the TBAOH treatment will induce hydrophobicity to the coating.

Analysis of the transition regions of RH (humidification and dehumidification) revealed that during the moistening (see Fig. 6b) the canvas coated with CNC had the lowest decrease of E'. However, during the dehumidification (see Fig. 6c), the CNC-coated canvas exhibited a strong decrease followed by an increase of the storage modulus, which was not so pronounced or even absent in all the other samples. From these results, it seems that before reaching a certain steady state, the canvas might have to experience several RH cycles, which would in practice be achieved in the early lifetime of the treatment. The reasons behind such behavior are complex, and it could be that an equilibrium in terms of moisture diffusion through the nanocellulose layer and the canvas has to be reached.

4 Conclusions

Canvas degradation is one of the crucial issues of easel paintings, which leads to their irreversible damage. In this work, we demonstrate for the first time that different types of natural cellulose nanomaterials have a potential for use as a mechanical reinforcement of degraded cellulosic canvases. Such treatments are also in line with the strategy of minimal intervention. The results show that nanocellulose can provide a substantial reinforcement in the low elongation region, *i.e.* below 3%, that is where strengthening should be provided. In this region, the stiffening effect of CNF, CCNF and CNC is much higher than that achieved using traditional wax-resin formulation (Beva 371). Despite the high porosity of the canvas, nanocelluose, irrespectively of the aspect ratio of the nanofibers, formed a film after deposition from a diluted suspension. The structure of the reinforcing film was markedly influenced by the aspect ratio of the nanocelluloses — short CNC formed a dense homogeneous layer, while longer CNF and CCNF yielded layered structures.

When comparing different types of nanocellulose, CCNF showed better performance per gained weight. However, it could only be handled at a low solids content, which means that the canvas was exposed to larger water volumes than with the other nanocelluloses. Attempts to reduce the sensitivity of CCNF to water by ionic cross-linking and by hydrophobization did not exhibit major improvements. CNC showed the smallest reinforcement per gained weight but the highest reinforcement per equivalent number of coatings, due to the possibility to use higher solids content in the aqueous dispersion. Moreover, CNC gave the lowest mechanical changes upon RH variations, which can be beneficial for further preservation of canvas upon storage. CNF compromised the mass uptake and the mechanical reinforcement and did not change the responsiveness of the treated canvas to humidity variations. Unlike CCNF and CNC, CNF does not

carry acidic chemical groups and therefore has a potential to have better long-term stability. On the other hand, when deacidification of the canvas is performed and a certain alkaline reserve is present, this acidic character of CCNF and CNC may not induce any problems. Acidity remains beyond the scope of this work and should be addressed by further research. Additionally, the dimensional changes of the canvas upon wetting and drying affected by deposition of nanocellulose suspensions should be studied.

Nanocellulose is similar in nature to cotton and is an attractive alternative to the synthetic polymers used today for canvas consolidation. Some of the other advantages are: no alteration of canvas color and low depth of impregnation Nanocellulose also has higher degree of crystallinity compared to canvas fibers, which may be a key towards long-term stability. Another crucial aspect is the reversibility of the treatment. The good film forming properties of the nanocelluloses on the surface of the canvas mean that there is limited penetration into the bulk of the canvas, thus providing potential for removing it if needed at a later stage.

Acknowledgements

This work has been performed in the frame of NANORESTART (NANOmaterials for the RESToration works of ART) project funded by Horizon 2020 European Union Framework Program for Research and Innovation (Grant Agreement No. 646063). The authors express their gratitude to RISE Bioeconomy (Sweden) and Stora Enso AB (Sweden) for providing the nanocellulose samples.

References

Ackroyd, P. (2002). The structural conservation of canvas paintings: changes in attitude and practice since the early 1970s. *Studies in Conservation*, *47*(sup1), 3–14. https://doi.org/10.1179/sic.2002.47.Supplement-1.3

Ackroyd, P., Phenix, A., & Villers, C. (2002). Not lining in the twenty-first century: Attitudes to the structural conservation of canvas paintings. *The Conservator*, *26*(1), 14–23. https://doi.org/10.1080/01410096.2002.9995172

ASTM D5034 − 09 (2013) Standard Test Method for Breaking Strength and Elongation of Textile Fabrics (Grab Test). (2013).

Berger, G. A. (1972). Formulating Adhesives for the Conservation of Paintings. *Studies in Conservation*, *17*(sup1), 613–629. https://doi.org/10.1179/sic.1972.17.s1.011i

Berger, G. A., & Russell, W. H. (1988). An evaluation of the preparation of canvas paintings using stress measurements. *Studies in Conservation*, *33*(4), 187–204. https://doi.org/10.1179/sic.1988.33.4.187

Berger, G. A., & Russell, W. H. (1990). Deterioration of Surfaces Exposed to Environmental Changes. *Journal of the American Institute for Conservation*, *29*(1), 45–76. https://doi.org/10.1179/019713690806046145

Bianco, L., Avalle, M., Scattina, A., Croveri, P., Pagliero, C., & Chiantore, O. (2015). A study on reversibility of BEVA®371 in the lining of paintings. *Journal of Cultural Heritage*, *16*(4), 479–485. https://doi.org/10.1016/j.culher.2014.09.001

Chelazzi, D., Chevalier, A., Pizzorusso, G., Giorgi, R., Menu, M., & Baglioni, P. (2014). Characterization and degradation of poly(vinyl acetate)-based adhesives for canvas paintings. *Polymer Degradation and Stability*, *107*, 314–320. https://doi.org/10.1016/j.polymdegradstab.2013.12.028

Dong, H., Snyder, J. F., Williams, K. S., & Andzelm, J. W. (2013). Cation-Induced Hydrogels of Cellulose Nanofibrils with Tunable Moduli. *Biomacromolecules*, *14*(9), 3338–3345. https://doi.org/10.1021/bm400993f

Dreyfuss-Deseigne, R. (2017). Nanocellulose Films in Art Conservation. *Journal of Paper Conservation*, *18*(1), 18–29. https://doi.org/10.1080/18680860.2017.1334422

Foster, G., Odlyha, M., & Hackney, S. (1997). Evaluation of the effects of environmental conditions and preventive conservation treatment on painting canvases. *Thermochimica Acta*, *294*(1), 81–89. https://doi.org/10.1016/S0040-6031(96)03147-4

Giorgi, R., Dei, L., Ceccato, M., Schettino, C., & Baglioni, P. (2002). Nanotechnologies for Conservation of Cultural Heritage: Paper and Canvas Deacidification. *Langmuir*, *18*(21), 8198–8203. https://doi.org/10.1021/la025964d

Habibi, Y., Lucia, L. A., & Rojas, O. J. (2010). Cellulose Nanocrystals: Chemistry, Self-Assembly, and Applications. *Chemical Reviews*, *110*(6), 3479–3500. https://doi.org/10.1021/cr900339w

Hedley, G. (1988). Relative humidity and the stress/strain response of canvas paintings: uniaxial measurements of naturally aged samples. *Studies in Conservation*, *33*(3), 133–148. https://doi.org/10.1179/sic.1988.33.3.133

Hendrickx, R., Desmarais, G., Weder, M., Ferreira, E. S. B., & Derome, D. (2016). Moisture uptake and permeability of canvas paintings and their components. *Journal of Cultural Heritage*, *19*, 445–453. https://doi.org/10.1016/j.culher.2015.12.008

Henriksson, M., Berglund, L. A., Isaksson, P., Lindström, T., & Nishino, T. (2008). Cellulose Nanopaper Structures of High Toughness. *Biomacromolecules*, *9*(6), 1579–1585. https://doi.org/10.1021/bm800038n

Iaccarino Idelson, A. (2009). About the choice of tension for canvas paintings. *CeROArt. Conservation, Exposition, Restauration d'Objets d'Art*, *4*.

Klemm, D., Heublein, B., Fink, H.-P., & Bohn, A. (2005). Cellulose: Fascinating Biopolymer and Sustainable Raw Material. *Angewandte Chemie International Edition*, *44*(22), 3358–3393. https://doi.org/10.1002/anie.200460587

Kolman, K., Nechyporchuk, O., Persson, M., Holmberg, K., & Bordes, R. (2017). Preparation of silica/polyelectrolyte complexes for textile strengthening applied to painting canvas restoration. *Colloids and Surfaces A: Physicochemical and Engineering Aspects*, *532*, 420–427. https://doi.org/10.1016/j.colsurfa.2017.04.051

Li, Q., Chen, W., Li, Y., Guo, X., Song, S., Wang, Q., … Zeng, J. (2016). Comparative study of the structure, mechanical and thermomechanical properties of cellulose nanopapers with different thickness. *Cellulose*, *23*(2), 1375–1382. https://doi.org/10.1007/s10570-016-0857-6

Mecklenburg, M. F. (1982). Some aspects of the mechanical behavior of fabric supported paintings. *National Museum Act*.

Mecklenburg, M. F. (2005). The structure of canvas supported paintings. In *International conference on painting conservation: canvases, behaviour, deterioration and treatment* (pp. 133–137). Valencia.

Mecklenburg, M. F., & Fuster Lopez, L. (2008). Failure mechanisms in canvas supported paintings: approaches for developing consolidation protocols. In *Colore e conservazione: materiali e metodi nel restauro delle opere policrome mobili: terzo congresso internazionale* (pp. 51–60). Il prato.

Mecklenburg, M. F., McCormick-Goodhart, M., & Tumosa, C. S. (1994). Investigation into the Deterioration of Paintings and Photographs Using Computerized Modeling of Stress Development. *Journal of the American Institute for Conservation*, *33*(2), 153–170. https://doi.org/10.2307/3179424

Michalski, S. (1991). Paintings - Their Response to Temperature, Relative Humidity, Shock, and Vibration. In M. Marion (Ed.), *Art in transit: Studies in the transport of paintings* (pp. 223–248). National Gallery of Art.

Moon, R. J., Martini, A., Nairn, J., Simonsen, J., & Youngblood, J. (2011). Cellulose nanomaterials review: structure, properties and nanocomposites. *Chemical Society Reviews*, *40*(7), 3941–3994. https://doi.org/10.1039/C0CS00108B

Nechyporchuk, O., Belgacem, M. N., & Bras, J. (2016). Production of cellulose nanofibrils: A review of recent advances. *Industrial Crops and Products*, *93*, 2–25. https://doi.org/10.1016/j.indcrop.2016.02.016

Nechyporchuk, O., Belgacem, M. N., & Pignon, F. (2016). Current progress in rheology of cellulose nanofibril suspensions. *Biomacromolecules*, *17*(7), 2311–2320. https://doi.org/10.1021/acs.biomac.6b00668

595 Nechyporchuk, O., Kolman, K., Oriola, M., Persson, M., Holmberg, K., & Bordes, R. (2017).
596 Accelerated ageing of cotton canvas as a model for further consolidation practices. *Journal*
597 *of Cultural Heritage*, *28*, 183–187. https://doi.org/10.1016/j.culher.2017.05.010
598 Nechyporchuk, O., Pignon, F., & Belgacem, M. N. (2015). Morphological properties of
599 nanofibrillated cellulose produced using wet grinding as an ultimate fibrillation process.
600 *Journal of Materials Science*, *50*(2), 531–541. https://doi.org/10.1007/s10853-014-8609-1
601 Nechyporchuk, O., Yu, J., Nierstrasz, V. A., & Bordes, R. (2017). Cellulose Nanofibril-Based
602 Coatings of Woven Cotton Fabrics for Improved Inkjet Printing with a Potential in E-Textile
603 Manufacturing. *ACS Sustainable Chemistry & Engineering*, *5*(6), 4793–4801.
604 https://doi.org/10.1021/acssuschemeng.7b00200
605 Oriola, M., Možir, A., Garside, P., Campo, G., Nualart-Torroja, A., Civil, I., … Strlič, M. (2014).
606 Looking beneath Dalí's paint: non-destructive canvas analysis. *Analytical Methods*, *6*(1),
607 86–96. https://doi.org/10.1039/C3AY41094C
608 Ploeger, R., René de la Rie, E., McGlinchey, C. W., Palmer, M., Maines, C. A., & Chiantore, O.
609 (2014). The long-term stability of a popular heat-seal adhesive for the conservation of
610 painted cultural objects. *Polymer Degradation and Stability*, *107*, 307–313.
611 https://doi.org/10.1016/j.polymdegradstab.2014.01.031
612 Rånby, B. G. (1949). Aqueous Colloidal Solutions of Cellulose Micelles. *Acta Chemica*
613 *Scandinavica*, *3*, 649–650. https://doi.org/10.3891/acta.chem.scand.03-0649
614 Roche, A. (1993). Influence du type de chassis sur le vieillissement mecanique d'une peinture sur
615 toile. *Studies in Conservation*, *38*(1), 17–24. https://doi.org/10.1179/sic.1993.38.1.17
616 Ryder, N. (1986). Acidity in canvas painting supports: Deacidification of two 20th century
617 paintings. *The Conservator*, *10*(1), 31–36. https://doi.org/10.1080/01410096.1986.9995015
618 Santos, S. M., Carbajo, J. M., Gómez, N., Quintana, E., Ladero, M., Sánchez, A., … Villar, J. C.
619 (2015). Use of bacterial cellulose in degraded paper restoration. Part I: application on model
620 papers. *Journal of Materials Science*, 1–12. https://doi.org/10.1007/s10853-015-9476-0

621 Shimizu, M., Saito, T., Fukuzumi, H., & Isogai, A. (2014). Hydrophobic, Ductile, and Transparent
622 Nanocellulose Films with Quaternary Alkylammonium Carboxylates on Nanofibril
623 Surfaces. *Biomacromolecules*, *15*(11), 4320–4325. https://doi.org/10.1021/bm501329v
624 Stachurski, Z. H. (1997). Deformation mechanisms and yield strength in amorphous polymers.
625 *Progress in Polymer Science*, *22*(3), 407–474. https://doi.org/10.1016/S0079-
626 6700(96)00024-X
627 Stoner, J. H., & Rushfield, R. (2012). *Conservation of Easel Paintings*. Routledge.
628 Turbak, A. F., Snyder, F. W., & Sandberg, K. R. (1983). Microfibrillated cellulose, a new cellulose
629 product: Properties, uses, and commercial potential. *Journal of Applied Polymer Science:*
630 *Applied Polymer Symposium*, *37*, 815–827.
631 Villers, C. (2004). Post minimal intervention. *The Conservator*, *28*(1), 3–10.
632 https://doi.org/10.1080/01410096.2004.9995197
633 Völkel, L., Ahn, K., Hähner, U., Gindl-Altmutter, W., & Potthast, A. (2017). Nano meets the sheet:
634 adhesive-free application of nanocellulosic suspensions in paper conservation. *Heritage*
635 *Science*, *5*, 23. https://doi.org/10.1186/s40494-017-0134-5
636 Wågberg, L., Decher, G., Norgren, M., Lindström, T., Ankerfors, M., & Axnäs, K. (2008). The
637 Build-Up of Polyelectrolyte Multilayers of Microfibrillated Cellulose and Cationic
638 Polyelectrolytes. *Langmuir*, *24*(3), 784–795. https://doi.org/10.1021/la702481v
639 Wu, S.-Q., Li, M.-Y., Fang, B.-S., & Tong, H. (2012). Reinforcement of vulnerable historic silk
640 fabrics with bacterial cellulose film and its light aging behavior. *Carbohydrate Polymers*,
641 *88*(2), 496–501. https://doi.org/10.1016/j.carbpol.2011.12.033
642 Young, C. (1999). Towards a better understanding of the physical properties of lining materials for
643 paintings: Interim results. *The Conservator*, *23*(1), 83–91.
644 https://doi.org/10.1080/01410096.1999.9995142

Young, C., & Jardine, S. (2012). Fabrics for the twenty-first century: As artist canvas and for the structural reinforcement of easel paintings on canvas. *Studies in Conservation*, *57*(4), 237–253. https://doi.org/10.1179/2047058412Y.0000000007

Graphical abstract

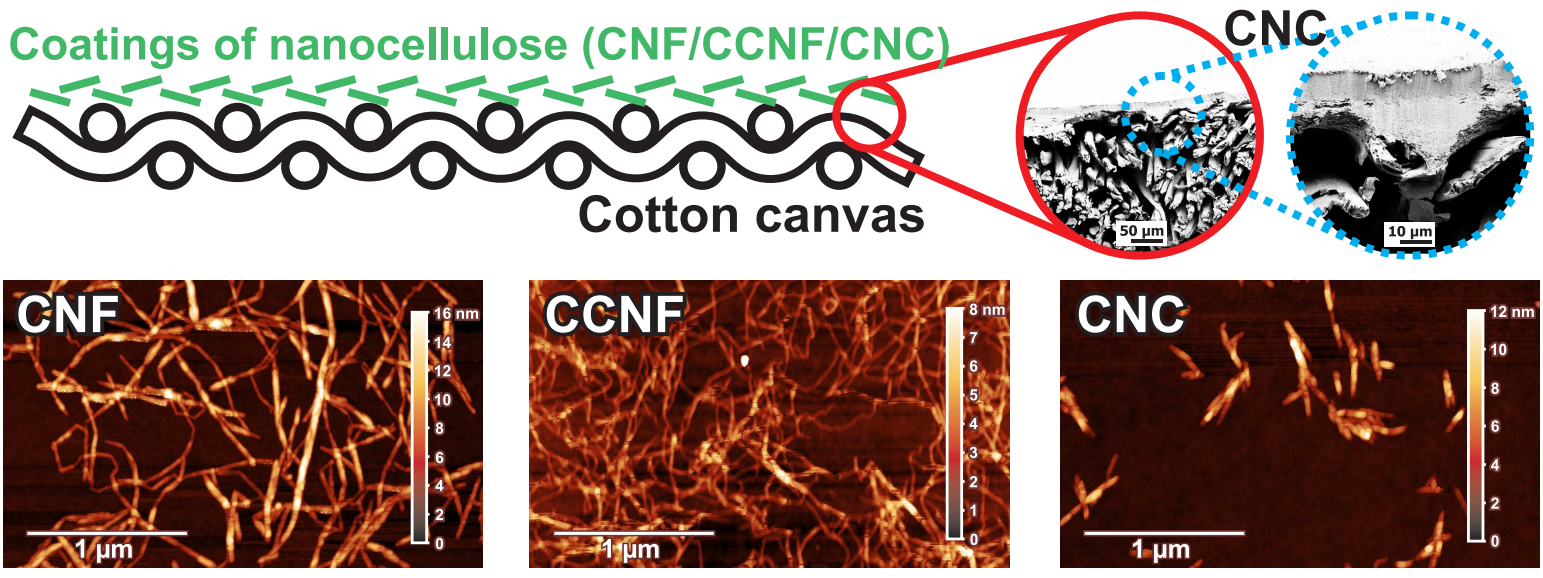

Figure 1

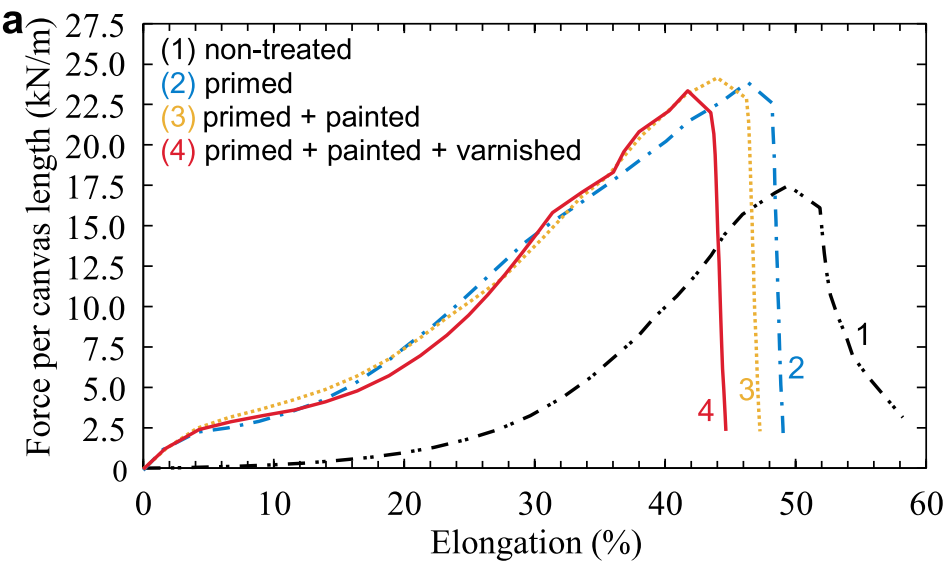
a
(1) non-treated
(2) primed
(3) primed + painted
(4) primed + painted + varnished
Force per canvas length (kN/m)
Elongation (%)
0
2.5
5.0
7.5
10.0
12.5
15.0
17.5
20.0
22.5
25.0
27.5
0
10
20
30
40
50
60
1
2
3
4

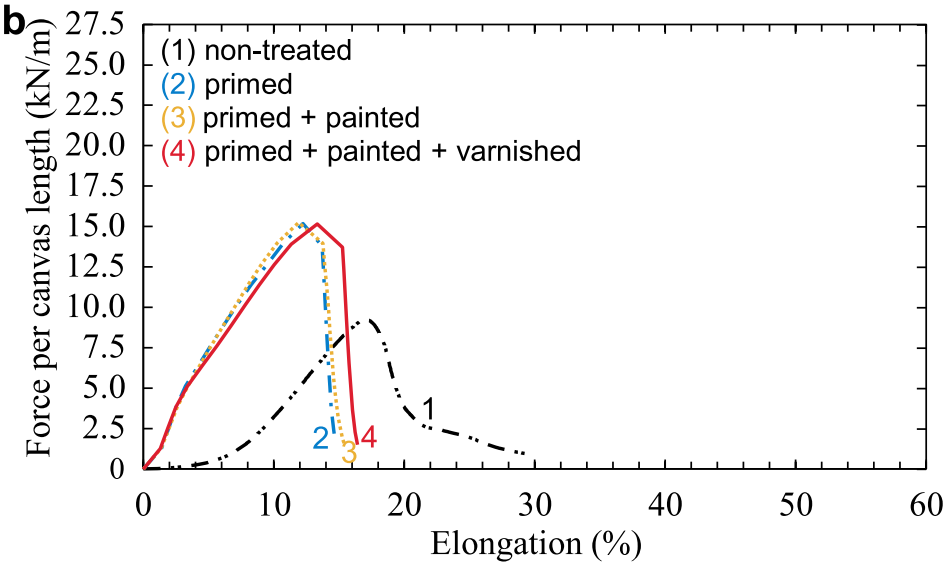
b
(1) non-treated
(2) primed
(3) primed + painted
(4) primed + painted + varnished
Force per canvas length (kN/m)
Elongation (%)
0
2.5
5.0
7.5
10.0
12.5
15.0
17.5
20.0
22.5
25.0
27.5
0
10
20
30
40
50
60
1
2
3
4

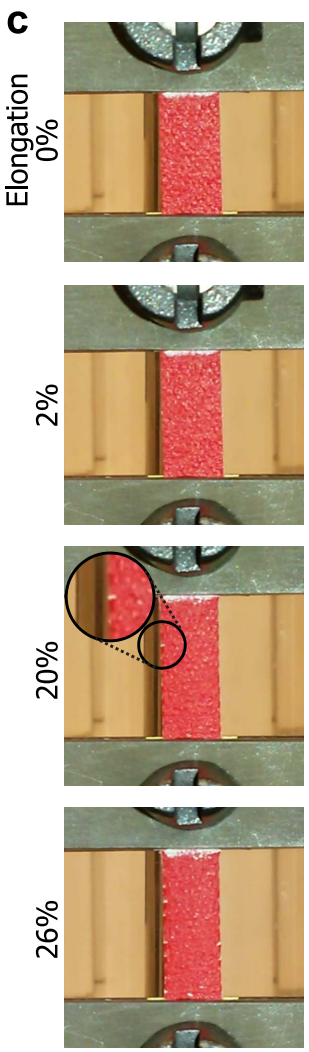
c
Elongation
0%
2%
20%
26%

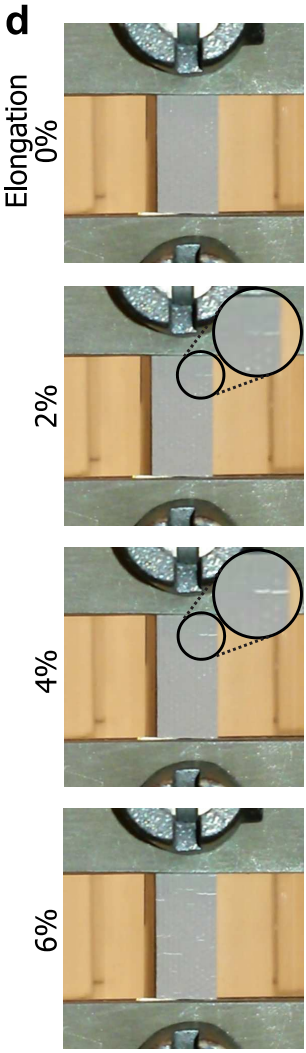
d
Elongation
0%
2%
4%
6%

Figure 2

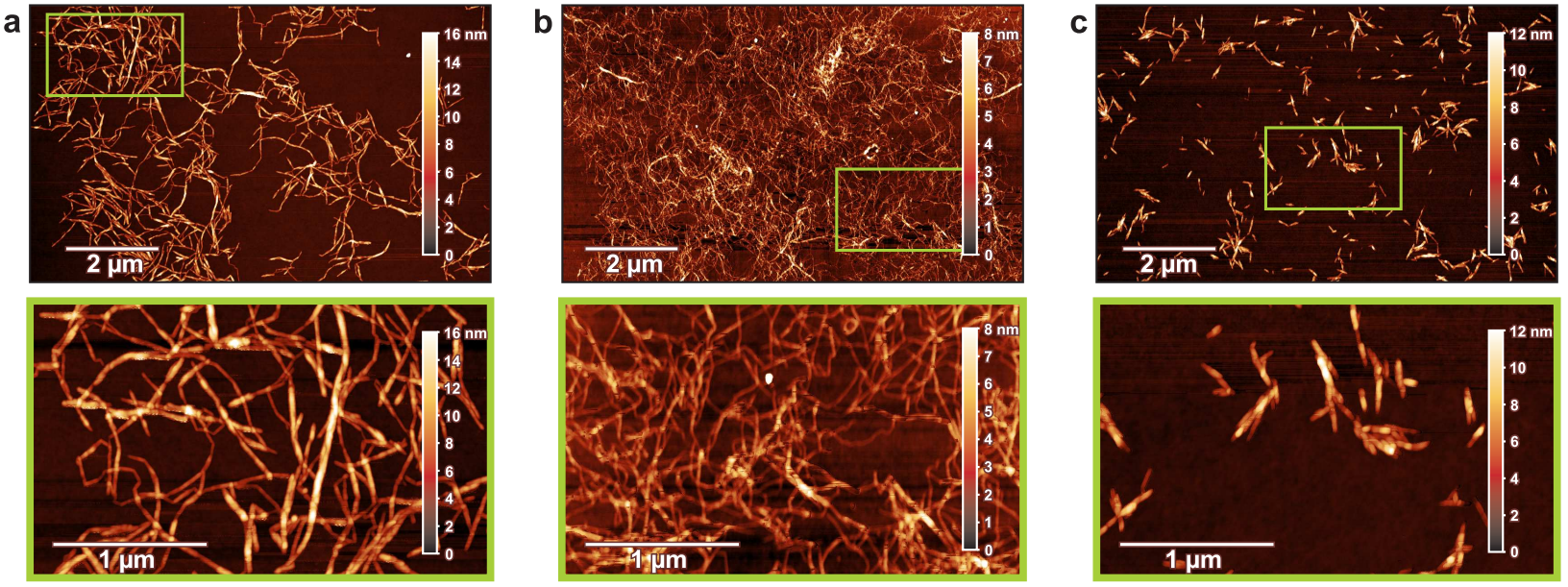
a
16 nm
14
12
10
8
6
4
2
0
2 µm
1 µm
b
8 nm
7
6
5
4
3
2
1
0
2 µm
1 µm
c
12 nm
10
8
6
4
2
0
2 µm
1 µm

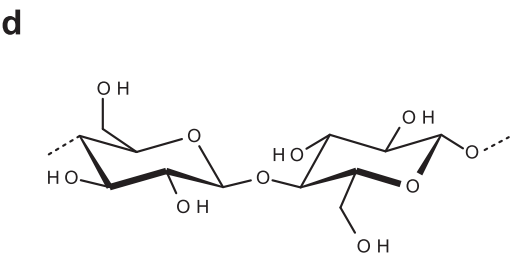
d
O H
O
H O
O H
O H
H O
O
O
O H

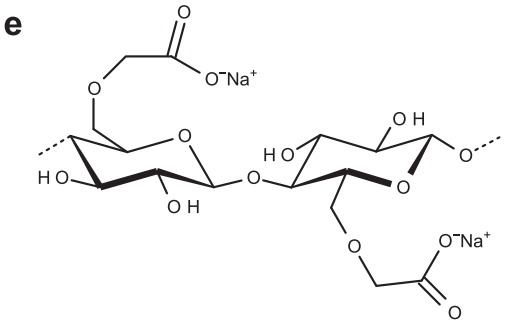
e
O
O
O⁻Na⁺
O
H O
O H
O H
H O
O
O
O
O⁻Na⁺
O

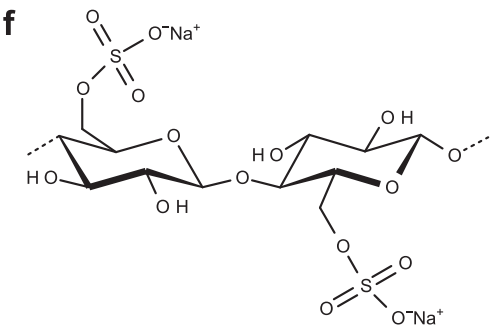
f
O
O⁻Na⁺
S
O
O
O H
O
H O
O H
O H
H O
O
O
O
S
O
O
O⁻Na⁺

Figure 3

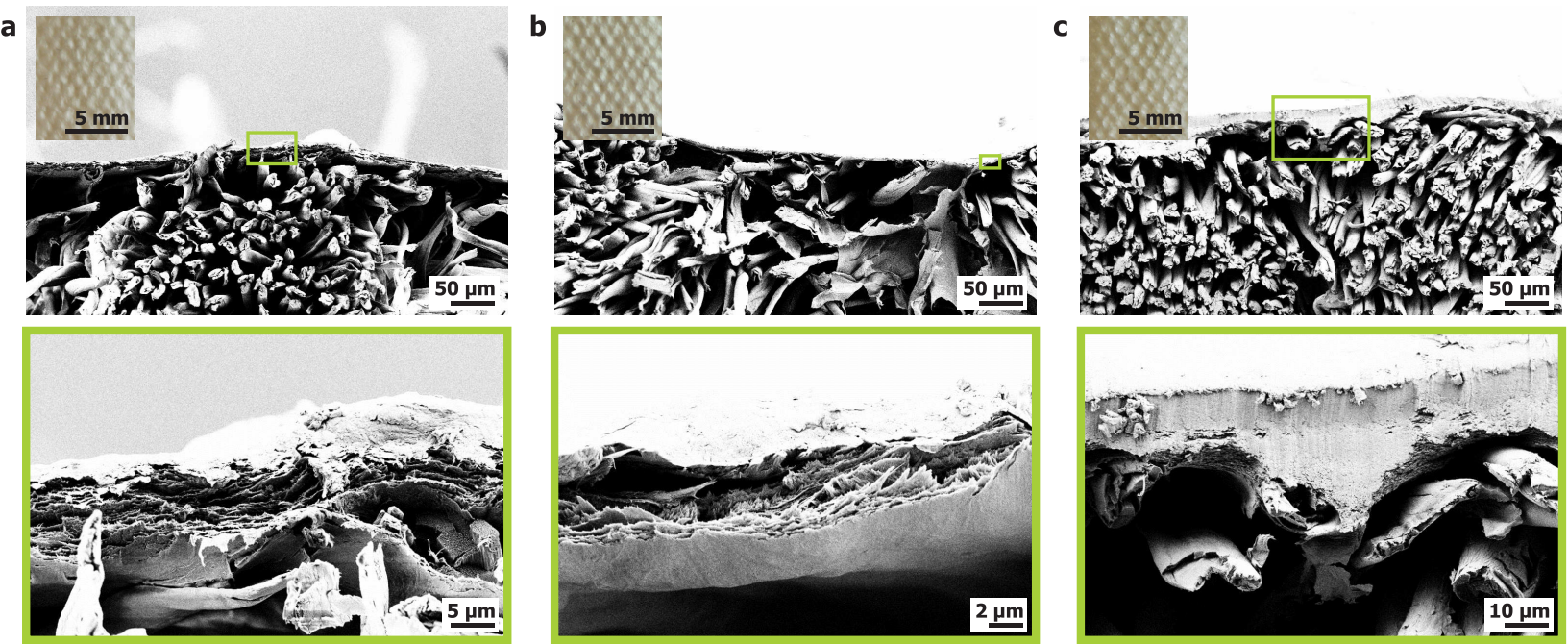

Figure 4

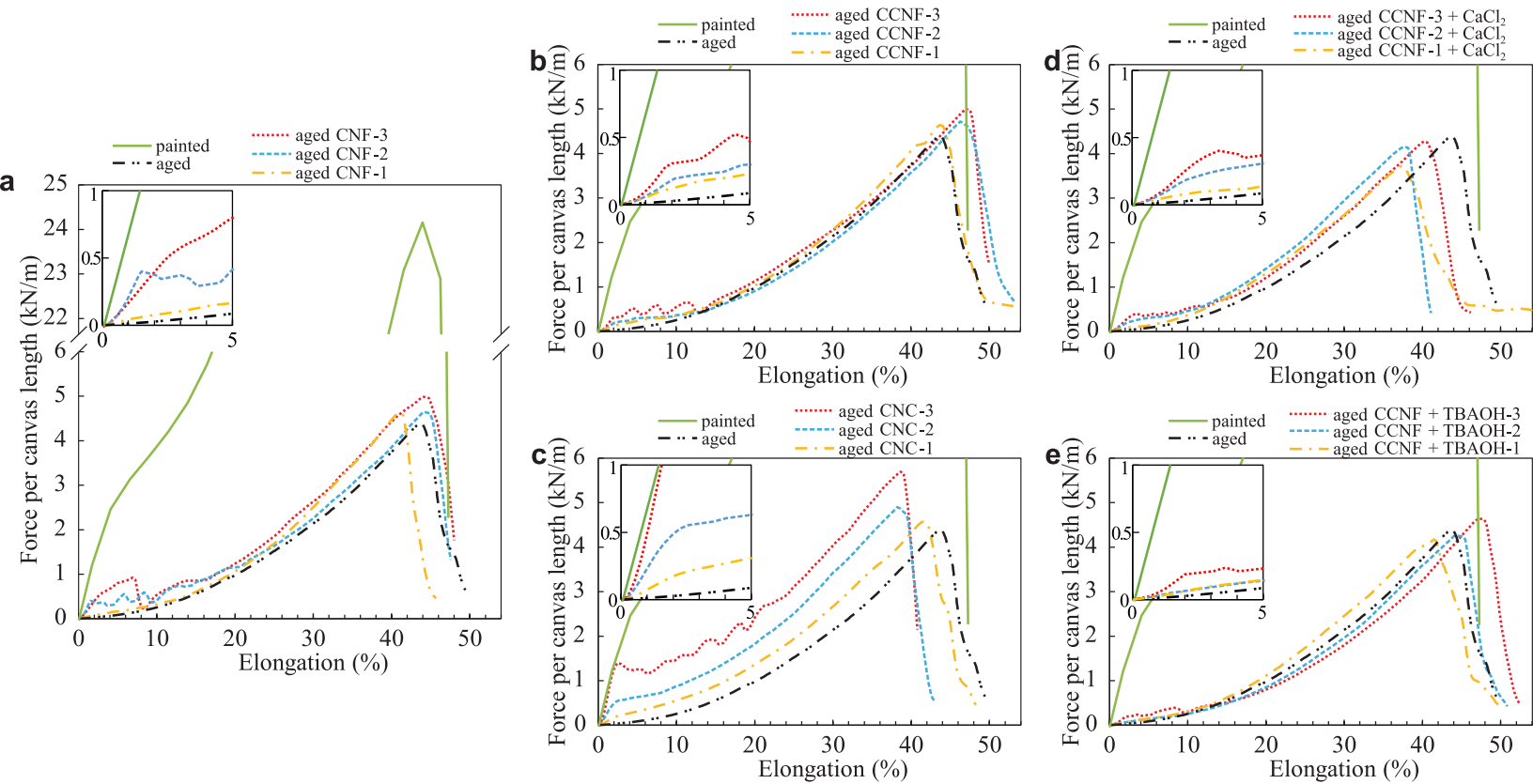
a
painted
aged
aged CNF-3
aged CNF-2
aged CNF-1
Force per canvas length (kN/m)
Elongation (%)
b
aged CCNF-3
aged CCNF-2
aged CCNF-1
c
aged CNC-3
aged CNC-2
aged CNC-1
d
aged CCNF-3 + CaCl2
aged CCNF-2 + CaCl2
aged CCNF-1 + CaCl2
e
aged CCNF + TBAOH-3
aged CCNF + TBAOH-2
aged CCNF + TBAOH-1

Figure 5

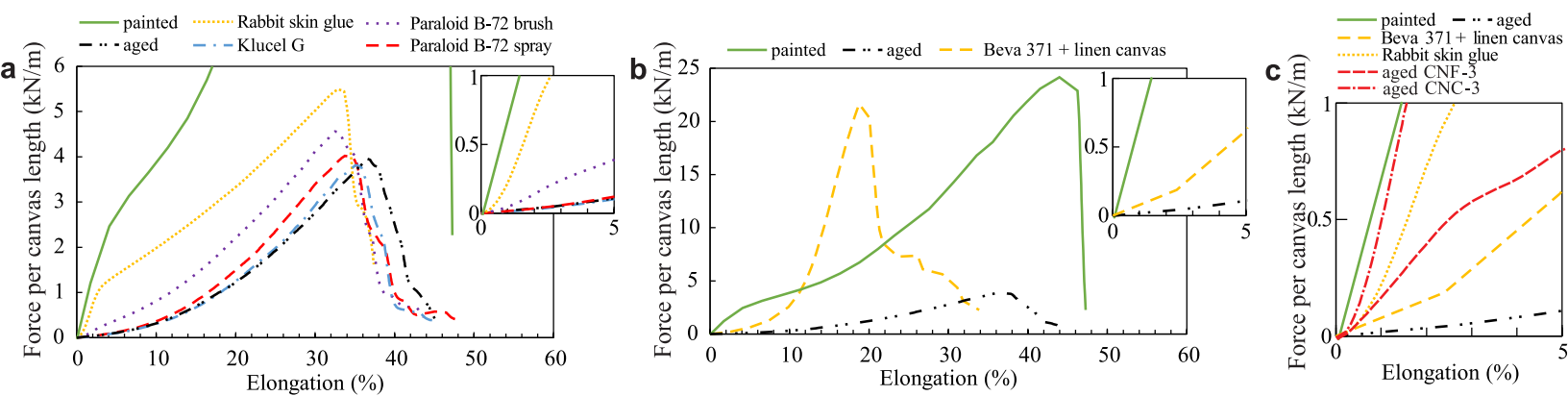
a
painted
aged
Rabbit skin glue
Klucel G
Paraloid B-72 brush
Paraloid B-72 spray
Force per canvas length (kN/m)
Elongation (%)
b
painted
aged
Beva 371 + linen canvas
Force per canvas length (kN/m)
Elongation (%)
c
painted
aged
Beva 371+ linen canvas
Rabbit skin glue
aged CNF-3
aged CNC-3
Force per canvas length (kN/m)
Elongation (%)

Figure 6

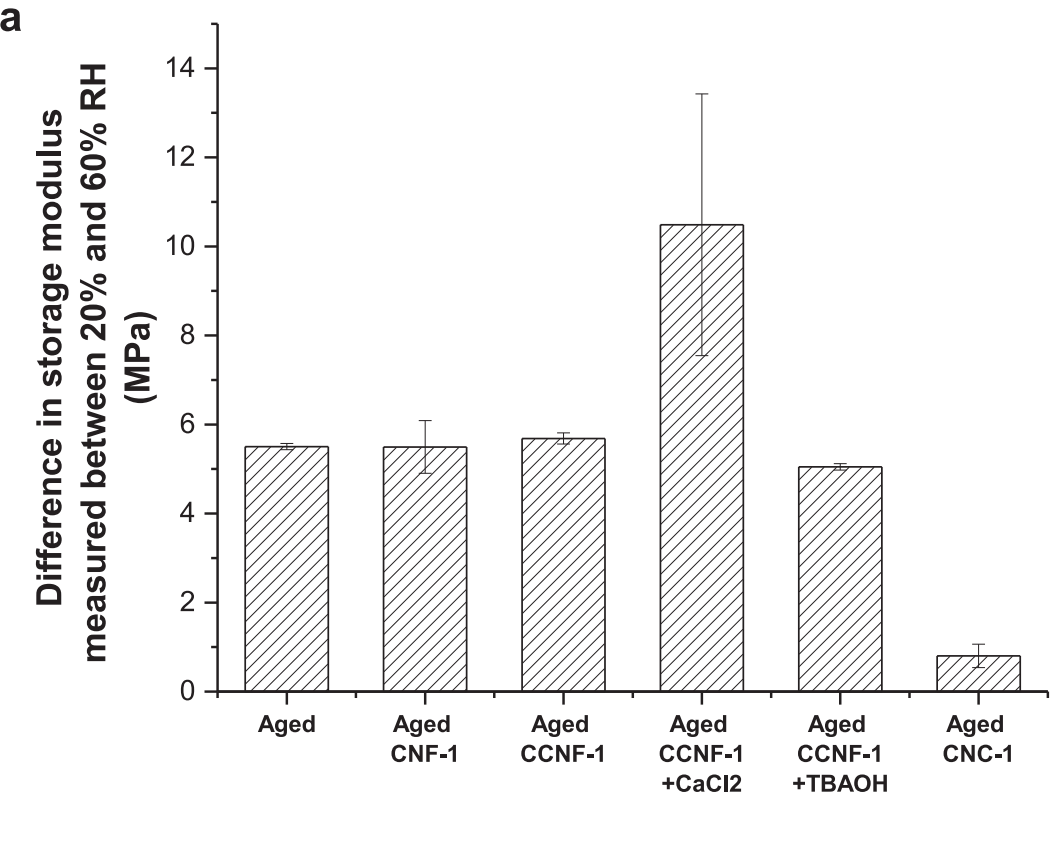
a
Difference in storage modulus measured between 20% and 60% RH (MPa)
0
2
4
6
8
10
12
14
Aged
Aged CNF-1
Aged CCNF-1
Aged CCNF-1 +CaCl2
Aged CCNF-1 +TBAOH
Aged CNC-1

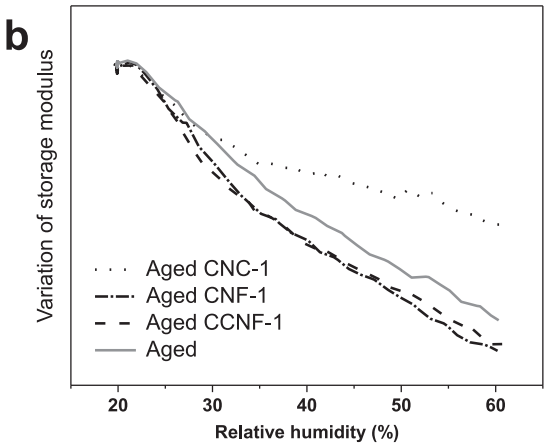
b
Variation of storage modulus
Aged CNC-1
Aged CNF-1
Aged CCNF-1
Aged
20
30
40
50
60
Relative humidity (%)

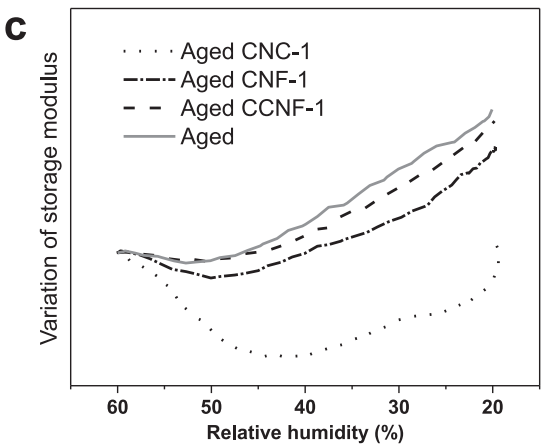
c
Variation of storage modulus
Aged CNC-1
Aged CNF-1
Aged CCNF-1
Aged
60
50
40
30
20
Relative humidity (%)